Elevated iron concentration in putamen and cortical speech motor network in developmental stuttering

Gabriel J. Cler[1], Saloni Krishnan[1,2], Daniel Papp[3], Charlotte E.E. Wiltshire[1], Jennifer Chesters[1], & Kate E. Watkins[1]

Abstract

Theoretical accounts of developmental stuttering implicate dysfunctional cortico-striatal-thalamo-cortical motor loops through the putamen. Analysis of conventional MRI brain scans in people who stutter has failed to yield strong support for this theory in terms of reliable differences in the structure or function of the basal ganglia, however. Here, we performed quantitative mapping of brain tissue, which can be used to measure iron content alongside markers sensitive to myelin and thereby offers particular sensitivity to the measurement of iron-rich structures such as the basal ganglia. Analysis of these quantitative maps in 41 men and women who stutter and 32 matched controls revealed significant group differences in maps of R2*, indicative of higher iron content in people who stutter than controls in the left putamen and in left hemisphere cortical regions important for speech motor control. Higher iron levels in brain tissue in people who stutter could reflect elevated dopamine levels or lysosomal dysfunction, both of which are implicated in stuttering. This study represents the first use of these quantitative measures in developmental stuttering and provides new evidence of microstructural differences in the basal ganglia and connected frontal cortical regions.

Author affiliations:

1 Wellcome Centre for Integrative Neuroimaging, Dept of Experimental Psychology, University of Oxford, OX2 6GG, Oxford, UK

2 Department of Psychology, Royal Holloway, University of London, Egham Hill, Surrey TW20 0EX

3 Wellcome Centre for Integrative Neuroimaging, FMRIB Centre, Nuffield Department of Clinical Neuroscience, University of Oxford, OX3 9DU, Oxford, UK

Correspondence to: Gabriel Cler
Dept of Experimental Psychology
University of Oxford
Oxford
UK
OX2 6GG
E-mail: gabriel.cler@psy.ox.ac.uk

Running title: Elevated iron in stuttering

Keywords: developmental stuttering; basal ganglia; iron; quantitative imaging

Abbreviations: CON=control; D2=Dopamine receptor 2; FA=Fractional anisotropy; FWHM=Full width at half maximum; IFG=inferior frontal gyrus; MPM=multi-parameter maps; MTsat=Magnetization transfer saturation; PD=Parkinson's disease; PWS=people who stutter; R1=longitudinal relaxation; R2*=effective transverse relaxation rate, equivalent to 1/T2*; ROI=region of interest; SSI=stuttering severity index; TFCE=threshold-free cluster enhancement; VBM=voxel-based morphometry.

Introduction

Developmental stuttering is characterized by dysfluent speech and is observed in 8% of children and ~1% of the general population.[1] Theoretical accounts of developmental stuttering implicate dysfunctional cortico-basal ganglia-thalamocortical motor circuits through the putamen.[2,3] Supportive evidence for this theory comes from observations of shared motor characteristics with basal ganglia disorders such as Parkinson's disease and dystonia, as well as changes to fluency in response to dopaminergic medication in people who stutter (PWS) or to deep brain stimulation.[2] Early positron-emission tomography (PET) studies indicated abnormal basal ganglia function during speech production and differences in dopamine metabolism in PWS. [4,5] However, recent meta-analyses that included functional MRI studies failed to identify dysfunction in these regions as either a state or trait characteristic of stuttering.[6] In terms of structure, conventional MRI data has been used in PWS to measure grey matter volume, cortical thickness, and diffusion properties of white matter fibre tracts. Whereas some consensus on the occurrence of white matter abnormalities has been reached, analysis of

cortical and subcortical volumes reveals inconsistent findings of grey matter differences in PWS.[6,7] In sum, even though there is strong theoretical evidence that points to basal ganglia dysfunction in developmental stuttering, imaging evidence to support or refute this theory is lacking.

In the current study, we scanned the brains of a large sample of PWS and a group of age- and gender-matched controls who do not stutter using a multi-parameter mapping (MPM)[8] protocol, which produces semi-quantitative whole-brain maps of three parameters: R1, MTsat, and R2*. These parameters reflect histologically-verified differences in tissue microstructure related to myelin and iron.[8,9] R1 (longitudinal relaxation) and MTsat (magnetization transfer saturation) are both correlated with the amount of myelin in grey and white matter.[9] R2* (effective transverse relaxation rate, equivalent to 1/T2*), is correlated with post-mortem estimates of iron deposits in grey matter.[10]

Iron is found in greatest concentration in the basal ganglia. Too little iron is considered detrimental during early development, and lower R2* in the basal ganglia is associated with poorer cognitive ability in adolescents.[11] On the other hand, greater iron concentration as indicated by higher R2* is a hallmark of Parkinson's disease[12] and increases with ageing.[13] We predicted, therefore, that this parameter would be sensitive to any previously undetected differences in the basal ganglia in PWS, but we did not have a directional hypothesis about whether R2* (iron concentration) would be higher or lower relative to controls.

Methods

Participants

Multi-parameter maps were acquired from 73 participants: 41 people who stutter (PWS, 9 women) and 32 controls (CON, 9 women). Data from an additional 18 people were excluded due to: acquisition error related to head placement (2 PWS, 1 CON); low image or map quality due to movement (8 PWS; 7 CON; see supplemental material). PWS were aged 19–45 years (median: 31.2), and CON were aged 19–44 (median: 28.6); the groups did not significantly differ in age ($t(64.4) = -1.5$, $p > 0.14$). Stuttering severity was assessed in PWS with the SSI-4 (Stuttering Severity Instrument - Fourth Edition, Riley, 2009). The men who stutter were scanned as part of a baseline session of a treatment study that required them to have at least a

mild/moderate score at screening (SSI ≥ 20). All participants met this criterion, but some had milder scores when re-tested during the baseline session, including one who was classed as very mild (SSI = 16). Thus, the final scores ranged from 16–40 (median: 25). Participants had no history of speech, language, or neurological conditions other than developmental stuttering. Participants provided written consent and were compensated for their participation. All procedures were approved by the University of Oxford ethics committee.

Quantitative Parameter Map Estimation and Analysis

Scans were acquired on a Siemens Prisma 3T scanner with three 3D multi-echo FLASH scans of predominantly T1 (T1w), proton density (PDw), and magnetization transfer (MTw) weighting, along with a B1 transmit field map and a B0 static field map.[8] A tailored pulse sequence was used: 1×1×1 mm resolution, FOV=256×224×176 mm^3, TR=25ms, bandwidth=488 Hz/pixels, first TE/echo spacing=2.3/2.3ms, 6° flip angle (PDw, MTw), or 21° (T1w), slab rotation=30°, and number of echoes=8 (PDw, MTw) or 6 (T1w), GRAPPA acceleration factor 2×2, 40 reference lines in each phase-encoded direction. B1 maps were acquired with SE and STE with a TR of 500ms, and TEs of 37.06ms (SE) and 68.28ms (STE). B0 maps were acquired with TR of 1020ms and TEs of 10 and 12.46ms.

Quantitative map estimation

The hMRI toolbox was used to calculate and process parameter maps of R1, MTsat, and R2* from the T1-, PD-, and MT-weighted images using the integrated pipeline with default settings.[9] Maps were segmented into grey and white matter and registered to MNI space. Segmented maps were smoothed with a 6-mm Gaussian FWHM (sigma=2.55). Importantly, all processing preserved the quantitative parameter values, without modulating for volume changes.[9] A schematic with images and maps from these steps for a single participant is shown in Figure 1.

Statistical analysis

Statistical analysis was performed using the FMRIB Software Library (FSL). For each map and tissue type (MTsat, R1, R2* × white, grey matter), a whole-brain general linear model analysis was performed using permutation testing with 5000 permutations. Statistical inference was drawn for the group contrasts of PWS>CON and CON>PWS using threshold-free cluster

enhancement (TFCE) to identify voxels in which the measurements between groups differed significantly. TFCE identifies regions of statistical difference without specifying an arbitrary cluster-forming height threshold; instead, small regions that are very different between groups or large regions with smaller differences may be identified, as long as they exhibit cluster-like regional specificity.[14] Significance was set at $p<.025$ to correct for the two single-tailed t-tests performed to assess group differences in both directions.[15]

The remaining statistical analyses were performed in R using analyses of variance (R version: 4.0.2; command: aov). Mean values of R2* were extracted for the statistical clusters in regions showing significant group differences to test relationships between R2* and age and compare these relationships between groups (age, group, and age × group as factors). Within the PWS group, the relationship to stuttering severity in these regions was tested statistically with R2* as the dependent measure and age, stuttering severity index, and age × stuttering severity as factors.

Results

PWS and CON did not differ in terms of whole brain volume or values averaged across all voxels in the grey and white tissue maps of R1, MTsat and R2* (Supplemental Table 1).

Whole-brain voxel-wise analysis of the quantitative maps revealed significantly higher grey matter R2* in PWS compared with CON subcortically in the left putamen, and cortically primarily in the left frontal lobe, including: the frontal opercular cortex extending to the anterior insula; the inferior frontal gyrus (pars opercularis) and posterior extent of the inferior frontal sulcus; and ventral precentral gyrus corresponding to the level of the representation of tongue movements[16] (see Table 1 and Figure 2A). It was striking that at this threshold ($p< .025$), the group differences were restricted to the left hemisphere. At a lower threshold of $p<.05$, group differences were also seen in the left caudate nucleus, subcortically, and more extensive portions of the right and left hemispheres, cortically (Supplemental Figure 1).

Mean R2* values for each significant cluster are shown for each participant (Figure 2B and C and Supplemental Table 2) and examined further against age (Supplemental Figure 2). As expected,[13] there was a significant linear increase in R2* with age in all regions, but importantly these relationships did not differ between groups (i.e., no interaction between group and age; Supplemental Table 2).

To check that the focal differences in grey matter R2* were not due to morphometric differences in PWS, we performed a voxel-based morphometry (VBM) analysis using standard T1-weighted images (see supplemental material). The groups were not different in terms of their relative amounts of grey matter anywhere in the brain.

In the PWS group, we examined if there was a significant relationship between stuttering severity and R2* controlling for age in any of the grey matter regions showing higher R2*; no regions showed a significant relationship between R2* and stuttering severity (Supplemental Table 3).

There were no differences between groups in the white matter R2* maps or in the grey or white matter maps of the myelin-sensitive markers, R1 and MTsat.

Discussion

Obtaining multi-parameter maps in a large cohort of people who do and do not stutter allowed us to conduct a detailed examination of neural microstructure, tied to histologically- and neurobiologically-relevant processes. Our results provide evidence of microstructural differences in people who stutter consistent with theoretical accounts of developmental stuttering that implicate dysfunction in cortico-basal ganglia-thalamocortical loops through the putamen.[2,3] Below we discuss these findings in the context of the relationships between iron in brain tissue and dopamine. We also discuss the link to lysosomal dysfunction, which is implicated in stuttering through the identification of causative mutations in related genes.

R2* differences in the putamen and cortical speech motor regions

The R2* parameter provided by the quantitative mapping protocol has known sensitivity to non-heme iron (that is, iron in the tissue rather than in blood), based on direct comparisons of R2* to histology in post-mortem brains with and without neurodegenerative diseases.[10,17] Iron in the brain is found in highest concentration in the basal ganglia.[13] For this reason, we predicted it would be sensitive to detecting differences in these nuclei in PWS. Accordingly, one region in the basal ganglia had higher R2* in PWS: the left putamen, which has previously been implicated in theoretical accounts of stuttering.[2,3] Wu and colleagues found increased dopaminergic activity in the left insula and putamen in a very small sample of PWS.[4] Another

PET study showed that treatment success in PWS was predicted by decreased regional cortical blood flow in the left putamen.[18]

In addition to this basal ganglia difference, there were several cortical regions showing higher R2* in PWS (Table 1), all of which are part of the speech motor network. These left hemisphere cortical areas in inferior frontal and ventral motor cortex show disfluency-related activity and are commonly underactive in PWS relative to controls (state and trait).[6] How the R2* differences in these brain regions relate to abnormal patterns of brain activity or to stuttering and other motor characteristics in PWS is as yet unknown. Our analyses failed to reveal relationships in any area with a standardized measure of stuttering severity.

Possible interpretations of higher R2*/iron concentration: dopamine and lysosomal dysfunction

One explanatory model for higher iron concentration in grey matter in PWS implicates dopamine. Iron and dopamine have complex interactions in the brain and must remain in a precise homeostatic balance for healthy function. Accordingly, increasing extracellular dopamine leads to higher intracellular iron levels, and when iron is introduced in the cell, D2 receptor protein concentrations increase.[19,20] A recent study in typically fluent speakers has suggested R2* as a correlate of pre-synaptic vesicular dopamine concentration.[21] Thus R2* increases seen here in PWS could be an indirect marker of excess dopamine levels. Developmental stuttering has been hypothesized to result from an excess of dopamine, although the evidence in support of this hypothesis from PET and pharmacological interventions is weak due to small sample sizes or side effects of the medication.[2,4,22] On the other hand, R2* is also increased in Parkinson's disease in which dopamine is depleted; there, it is thought that the increased iron may be the causative agent that leads to the death of dopaminergic neurons in the substantia nigra.[23] This mechanism is related to lysosomal dysfunction, which is also implicated in stuttering and forms the basis of our second explanatory model for the increased iron concentration in PWS.

In typical function, lysosomes degrade and recycle cellular waste, repair plasma membranes, and decompose intracellular stores of ferritin (Fe^{3+}) into Fe^{2+} to be transported for cellular processes requiring iron ions.[24] Accordingly, lysosomal storage disorders can result in an accumulation of substrates that are otherwise typically decomposed or transported. One such

disorder, Gaucher disease, leads to an accumulation of iron in the brain and body. The genetic mutation that causes Gaucher disease is homozygous; when that same mutation is heterozygous, individuals have an increased risk of developing Parkinson's disease.[25] Heterozygous causative mutations in *GNPTAB, GNPTG,* and related genes have been identified in PWS, accounting for ~10% of PWS.[26] Homozygous mutations in these genes result in dysfunctions in intracellular trafficking and lysosomal processes.[26] Expression patterns of these genes in the Allen Human Brain Atlas are spatially coincident with the cortical networks showing differences in PWS and are particularly high in the frontal opercular cortex, where we found significantly higher concentrations of iron in PWS.[27] We therefore posit that the increased iron could be indicative of lysosomal dysfunction. We found that R2* increased with age, as expected,[13] but increases were not accelerated in PWS (no significant interaction between age and group, Supplemental Table 2). Thus it is possible that heterozygous lysosomal mutations in stuttering cause dysfunction at a critical period in development or lead to lysosomal dysfunction resulting in greater iron deposition that does not accumulate at a faster rate over time.

No differences in myelin markers or grey matter volume

Despite our reasonably large sample size, our analysis did not detect group differences in the other parameters provided by the quantitative maps or in grey matter volume. No differences were found in MTsat or R1 maps, both of which are thought to be sensitive to differences in the amount of myelin in a given area.[9] This result may appear inconsistent with the results of many diffusion weighted imaging studies in PWS (including our own), which reported lower fractional anisotropy (FA) in white matter tracts.[7] Lower FA could reflect a number of differences in white matter microstructure, including the orientation or dispersion of fibres in a voxel, axonal calibre and density, and not only the amount of myelin. We speculated previously that lower FA in PWS in some areas reflected differences in fibre organization, rather than amount of myelin.[28] The current results are consistent with that interpretation. Nevertheless, further studies are warranted to understand the relationships among these different measures of microstructure.

VBM has previously been used to examine whether regional amounts of grey matter differ in PWS relative to control groups.[7] The findings are equivocal: in some studies, PWS have more grey matter, in others less, and in others no group differences are reported. We found no

significant differences in amounts of grey matter in any brain region, and thus find no evidence that the R2* differences are related to differing amounts of grey matter in PWS.

This is the first study using multi-parameter mapping to measure R2*, R1, or MTsat in PWS. Even though it is in quite a large cohort (41 PWS, 32 CON), these novel results need to be replicated. One recent study has indicated similar findings in regards to iron using ultrasound to reveal elevated iron accumulation in the substantia nigra in PWS.[29] Here we similarly conclude that there are iron differences in the basal ganglia (and connected cortical areas) in PWS, although our analyses revealed no significant differences in iron levels in the substantia nigra. Further analyses are warranted and measurement using ultrasound in the same participants would clarify the current discrepancy between the results of the two studies.

Conclusion

In this study of a large sample of PWS, we provide evidence for elevated R2* in the left putamen and connected frontal cortical regions. This difference in R2* most likely reflects increased iron concentrations, which may be indicative of excess dopamine levels or lysosomal dysfunction in PWS. Further work is needed to link R2* differences to genetic profiles associated with developmental stuttering, to increased dopamine or lysosomal dysfunction, or to another neurobiological function that could point toward effective therapies for those who want them.

Acknowledgements

The authors would like to thank Dr. Martina Callaghan of University College London for the multi-parameter mapping sequence code. We would also like to thank Máiréad Healy and Louisa Needham for their assistance in data collection, along with members of the OHBA centre MRI team: Juliet Semple, Nicky Aikin, and Nicola Filippini. Our sincerest thanks also go to all of the participants who took part in this study.

Funding

This work was funded by the Medical Research Council (MR/N025539/1) and the National Institutes of Health - National Institute on Deafness and Other Communication Disorders (F32

DC017637) and supported by the NIHR Oxford Health Biomedical Research Centre. The Wellcome Centre for Integrative Neuroimaging is supported by core funding from the Wellcome Trust [203139/Z/16/Z].

Competing interests

The authors report no competing interests.

Supplementary material

Map quality assessment

Map quality was assessed using visual inspection and quantitative quality measures. All maps from 91 participants were visually inspected and images with acquisition errors were excluded (2 PWS, 1 CON). We calculated the coefficient of variation (CoV) within the segmented white matter and grey matter quantitative maps.[30] Visual inspection of the data distribution of the CoV within the R1 map revealed an obvious cutoff at 0.18 (see Supplemental Figure 3). Data for all maps from participants with R1 CoV values above this threshold were removed (8 PWS; 7 CON). The hMRI toolbox also automatically provides quality assessment measures representing motion during the initial scans;[9] the CoV measure is an assessment of the quality of the final parameter maps. For inter-scan motion, total translation was calculated as the Euclidean distance from the origin to the coregistration X,Y,Z (in mm) provided by the toolbox of MTw to PDw; coregistration T1w to PDw. For intra-scan motion, we compared standard deviation in white matter of the R2* maps (SD-R2*), calculated from each individual multi-echo acquisition (PDw, T1w, MTw). These are differentiated from the final R2* maps used in the statistical analyses, as those are generated from all three acquisitions and then combined via ESTATICS.[9] Data from all participants who were outliers on these five inter- and intra-scan motion measures (by visual inspection and statistically >3.5 SD from the mean on any of five automated measures: coregistration MTw to PDw; coregistration T1w to PDw; SD-R2* from MTw; SD-R2* from PDw; SD-R2* from T1w) were already excluded based on the CoV measure. Thus, data from the remaining 73 participants were included in all further analyses.

VBM Analysis

To ensure that quantitative differences in parameter maps of grey matter were not due to morphometric group differences, we also performed a voxel-based morphometry (VBM) analysis using standard MPRAGE images. High-resolution T1-weighted structural images were acquired alongside the quantitative parameter acquisitions with an MPRAGE protocol (PAT2, 1mm isotropic, TR/TE = 2400/3.98). There were 38 PWS and 27 CON in this analysis, as there were no standard MPRAGE images acquired in the first eight participants. Images were analysed with FSL-VBM, wherein images were brain-extracted, grey matter-segmented, and registered to MNI152 standard space using non-linear registration. The resulting images were averaged and flipped along the x-axis to create a left-right symmetric, study-specific grey matter template using an equal number of PWS and CON (27 PWS participants were selected at random and combined with data from 27 CON). All original grey matter images were non-linearly registered to this study-specific template and modulated to correct for local expansion or contraction due to the non-linear component of the spatial transformation. The modulated grey matter images were then smoothed with an isotropic Gaussian kernel with a sigma of 3 (~7mm FWHM). Images were statistically analysed identically to the parameter maps: a voxel-wise general linear model was applied using permutation-based non-parametric testing, correcting for multiple comparisons across space. Statistical inference was drawn for the group contrasts of PWS>CON and CON>PWS using threshold-free cluster enhancement at $p<.05$ to identify voxels in which the measurements between groups differed significantly.

No significant differences were found when correcting for multiple comparisons across space. Since the purpose of our VBM analysis was to confirm that the quantitative differences in R2* were not explained by morphometric differences in the cortex or subcortical grey matter, we lowered the threshold to uncorrected $p<.05$ ($t>2.1$) in the regions with elevated R2* in PWS. While none of the regions with sub-threshold VBM differences overlapped those with R2* differences, two regions of nearby cortex showed morphometric differences: (i) PWS had more grey matter in the most ventral extent of the post-central sulcus, just dorsal to the portion of central opercular cortex with higher R2* (MNI: [-56 -19 23], t=3.95, $p_{uncorr}<.0006$); (ii) PWS had more grey matter in cortex adjacent and posterior to the portion of inferior frontal sulcus with higher R2* (MNI: [-46 2 30], t=3.48, $p_{uncorr}<.002$). We conclude that differences in R2* are not explained by or overlapping with differences in the amount of grey matter.

References

1. Yairi E, Ambrose N. Epidemiology of stuttering: 21st century advances. *J Fluency Disord*. 2013;38(2):66-87. doi:10.1016/j.jfludis.2012.11.002
2. Alm PA. Stuttering and the basal ganglia circuits: A critical review of possible relations. *J Commun Disord*. 2004;37(4):325-369. doi:10.1016/J.JCOMDIS.2004.03.001
3. Chang S-E, Guenther FH. Involvement of the Cortico-Basal Ganglia-Thalamocortical Loop in Developmental Stuttering. *Front Psychol*. 2020;10:28. doi:10.3389/fpsyg.2019.03088
4. Wu JC, Maguire G, Riley G, et al. Increased dopamine activity associated with stuttering. *Neuroreport*. 1997;8(3):767-770. doi:10.1097/00001756-199702100-00037
5. Fox PT, Ingham RJ, Ingham JC, et al. A PET study of the neural systems of stuttering. *Nature*. 1996;382(6587):158-162.
6. Neef NE, Anwander A, Friederici AD. The Neurobiological Grounding of Persistent Stuttering: from Structure to Function. *Curr Neurol Neurosci Rep*. 2015;15(9):63. doi:10.1007/s11910-015-0579-4
7. Etchell AC, Civier O, Ballard KJ, Sowman PF. A systematic literature review of neuroimaging research on developmental stuttering between 1995 and 2016. *J Fluency Disord*. 2018;55:6-45. doi:10.1016/j.jfludis.2017.03.007
8. Weiskopf N, Suckling J, Williams G, et al. Quantitative multi-parameter mapping of R1, PD*, MT, and R2* at 3T: A multi-center validation. *Front Neurosci*. 2013. doi:10.3389/fnins.2013.00095
9. Tabelow K, Balteau E, Ashburner J, et al. hMRI – A toolbox for quantitative MRI in neuroscience and clinical research. *Neuroimage*. 2019;194:191-210. doi:10.1016/j.neuroimage.2019.01.029
10. De Barros A, Arribarat G, Combis J, Chaynes P, Péran P. Matching Ex vivo MRI with iron histology: Pearls and pitfalls. *Front Neuroanat*. 2019;13:68. doi:10.3389/fnana.2019.00068
11. Larsen B, Bourque J, Moore XTM, et al. Longitudinal development of brain iron is linked to cognition in youth. *J Neurosci*. 2020;40(9):1810-1818. doi:10.1523/JNEUROSCI.2434-19.2020
12. Wallis LI, Paley MNJ, Graham JM, et al. MRI assessment of basal ganglia iron deposition in Parkinson's disease. *J Magn Reson Imaging*. 2008. doi:10.1002/jmri.21563

13. Daugherty AM, Raz N. Appraising the Role of Iron in Brain Aging and Cognition: Promises and Limitations of MRI Methods. *Neuropsychol Rev*. 2015;25(3):272-287. doi:10.1007/s11065-015-9292-y
14. Smith SM, Nichols TE. Threshold-free cluster enhancement: Addressing problems of smoothing, threshold dependence and localisation in cluster inference. *Neuroimage*. 2009;44(1):83-98. doi:10.1016/j.neuroimage.2008.03.061
15. Chen G, Cox RW, Glen DR, Rajendra JK, Reynolds RC, Taylor PA. A tail of two sides: Artificially doubled false positive rates in neuroimaging due to the sidedness choice with t-tests. *Hum Brain Mapp*. 2019;40(3):1037-1043. doi:10.1002/hbm.24399
16. Eichert N, Watkins K, Mars R, Petrides M. Morphological and functional variability in central and subcentral motor cortex of the human brain. *Brain Struct Funct*. October 2020. doi:10.1101/2020.03.17.995035
17. Schenck JF. Magnetic resonance imaging of brain iron. *J Neurol Sci*. 2003;207(1-2):99-102. doi:10.1016/S0022-510X(02)00431-8
18. Ingham RJ, Wang Y, Ingham JC, Bothe AK, Grafton ST. Regional brain activity change predicts responsiveness to treatment for stuttering in adults. *Brain Lang*. 2013;127(3):510-519. doi:10.1016/j.bandl.2013.10.007
19. Dichtl S, Haschka D, Nairz M, et al. Dopamine promotes cellular iron accumulation and oxidative stress responses in macrophages. *Biochem Pharmacol*. 2018;148:193-201. doi:10.1016/j.bcp.2017.12.001
20. Unger EL, Wiesinger JA, Hao L, Beard JL. Dopamine D2 Receptor Expression Is Altered by Changes in Cellular Iron Levels in PC12 Cells and Rat Brain Tissue. *J Nutr*. 2008;138(12):2487-2494. doi:10.3945/jn.108.095224
21. Larsen B, Olafsson V, Calabro F, et al. Maturation of the human striatal dopamine system revealed by PET and quantitative MRI. *Nat Commun*. 2020;11(1):1-10. doi:10.1038/s41467-020-14693-3
22. Maguire GA, Nguyen DL, Simonson KC, Kurz TL. The Pharmacologic Treatment of Stuttering and Its Neuropharmacologic Basis. *Front Neurosci*. 2020;14. doi:10.3389/fnins.2020.00158
23. Funke C, Schneider SA, Berg D, Kell DB. Genetics and iron in the systems biology of Parkinson's disease and some related disorders. *Neurochem Int*. 2013;62(5):637-652. doi:10.1016/j.neuint.2012.11.015
24. Rouault TA. Iron on the brain. *Nat Genet*. 2001;28(4):299-300. doi:10.1038/91036
25. Bras JM. Lysosomal Storage Disorders and Iron. In: *International Review of*

Neurobiology. Vol 110. Academic Press Inc.; 2013:251-275. doi:10.1016/B978-0-12-410502-7.00012-0

26. Frigerio-Domingues C, Drayna D. Genetic contributions to stuttering: the current evidence. *Mol Genet Genomic Med*. 2017;5(2):95-102. doi:10.1002/mgg3.276
27. Benito-Aragón C, Gonzalez-Sarmiento R, Liddell T, et al. Neurofilament-lysosomal genetic intersections in the cortical network of stuttering. *Prog Neurobiol*. 2020;184:101718. doi:10.1016/j.pneurobio.2019.101718
28. Connally EL, Ward D, Howell P, Watkins KE. Disrupted white matter in language and motor tracts in developmental stuttering. *Brain Lang*. 2014;131:25-35. doi:10.1016/J.BANDL.2013.05.013
29. Liman J, Wolff von Gudenberg A, Baehr M, Paulus W, Neef NE, Sommer M. Enlarged Area of Mesencephalic Iron Deposits in Adults Who Stutter. *Front Hum Neurosci*. 2021;15:53. doi:10.3389/fnhum.2021.639269
30. Papp D, Callaghan MF, Meyer H, Buckley C, Weiskopf N. Correction of inter-scan motion artifacts in quantitative R1 mapping by accounting for receive coil sensitivity effects. *Magn Reson Med*. 2016;76(5):1478-1485. doi:10.1002/mrm.26058

Figure legends

Figure 1. Schematic of processing pipeline. Data from one participant shown through each stage of processing, with acquisition (MTw, PDw, and T1w images in native space) followed by processing in the hMRI toolbox running in SPM: map estimation (using MTw, PDw, and T1w images to calculate MTsat, R1, and R2* maps), map segmentation into separate grey and white matter tissue (calculated from MTsat and applied to all maps), warping maps to standard space (calculated from MTsat and applied to all maps), and smoothing. R1 and R2* values are in units of 1/seconds; MTsat are percent units (p.u.). Colormaps are scaled per parameter to show variation in grey matter.

Figure 2. Areas with higher R2* in people who stutter relative to controls. (**A**) Coloured overlay is the statistical map showing areas with higher R2* in PWS than controls (thresholded at $p<.025$) on top of the average MTsat map for all participants aligned to MNI space. Individual data for mean R2* plotted against age by group in (**B**) left putamen (**C**) left frontal operculum and insula. Red is PWS; black is CON. Circles are men and triangles are women. Shaded areas show 95% confidence intervals. In boxplots, centre line is median and edges are 25^{th} and 75^{th} percentiles. Abbrev: L: left hemisphere; preCG: precentral gyrus; IFS: Inferior frontal sulcus (posterior); IFGpo: Inferior frontal gyrus, pars opercularis; FO & INS: Frontal operculum / insula

Supplemental Figure 1. Subthreshold areas with higher R2* in people who stutter relative to controls. Coloured overlay is the statistical map showing areas with higher R2* in PWS than controls in red-to-yellow thresholded at corrected p<.05. Statistically significant areas at a corrected threshold of p<.025 are outlined in black. Shown on top of the average MTsat map for all participants aligned to MNI space. L: left; R: right hemispheres.

Supplemental Figure 2. Age and group effects on R2* in all areas with higher R2* in PWS than controls (p< .025). Associated statistical results are shown in Supplemental Table 2. Red is PWS; black is CON. Circles are men and triangles are women. Shaded areas show 95% confidence intervals. (A) L Superior frontal sulcus; (B) L Inferior frontal gyrus, pars opercularis; (C) L Inferior frontal sulcus (posterior); (D) L Putamen (same as Figure 2D); (E) L Frontal operculum / insula (same as Figure 2E); (F) L Precentral gyrus (ventral) ; (G) L planum temporale; (H) L Superior parietal lobule.

Supplemental Figure 3. Results of semi-automated quality control algorithm. CON shown in black on left; PWS shown in red on right. Circles are men and triangles are women. Quality control cutoff (dashed horizontal line) was chosen empirically to be consistent between groups and to separate acceptable from unacceptable movement. Only participants with grey matter covariance in R1 map ≤ .18 were included in all subsequent analyses. Data from three additional participants with acquisition artefacts were excluded and not shown here.

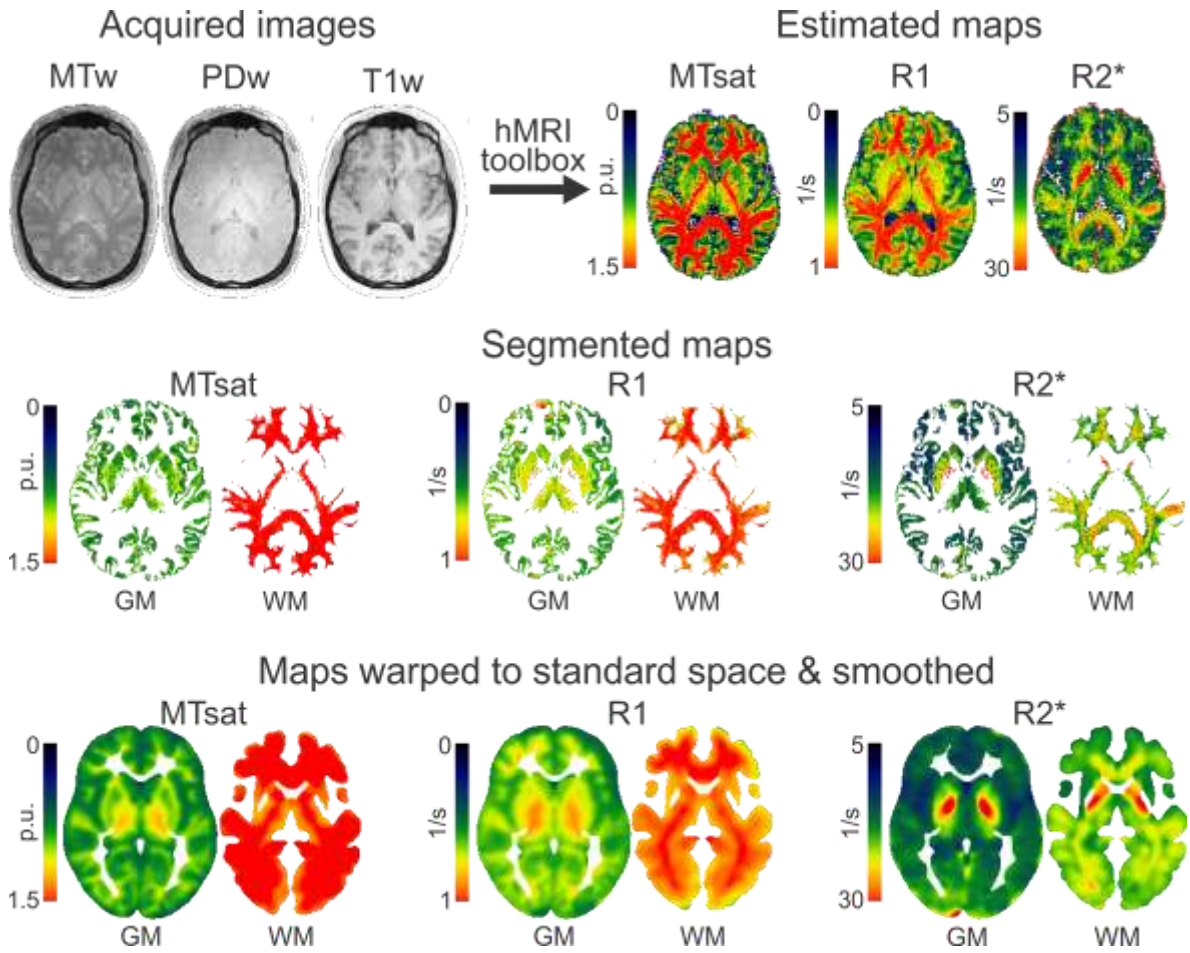

Figure 1. **Schematic of processing pipeline.** Data from one participant shown through each stage of processing, with acquisition (MTw, PDw, and T1w images in native space) followed by processing in the hMRI toolbox running in SPM: map estimation (using MTw, PDw, and T1w images to calculate MTsat, R1, and R2* maps), map segmentation into separate grey and white matter tissue (calculated from MTsat and applied to all maps), warping maps to standard space (calculated from MTsat and applied to all maps), and smoothing. R1 and R2* values are in units of 1/seconds; MTsat are percent units (p.u.). Colormaps are scaled per parameter to show variation in grey matter.

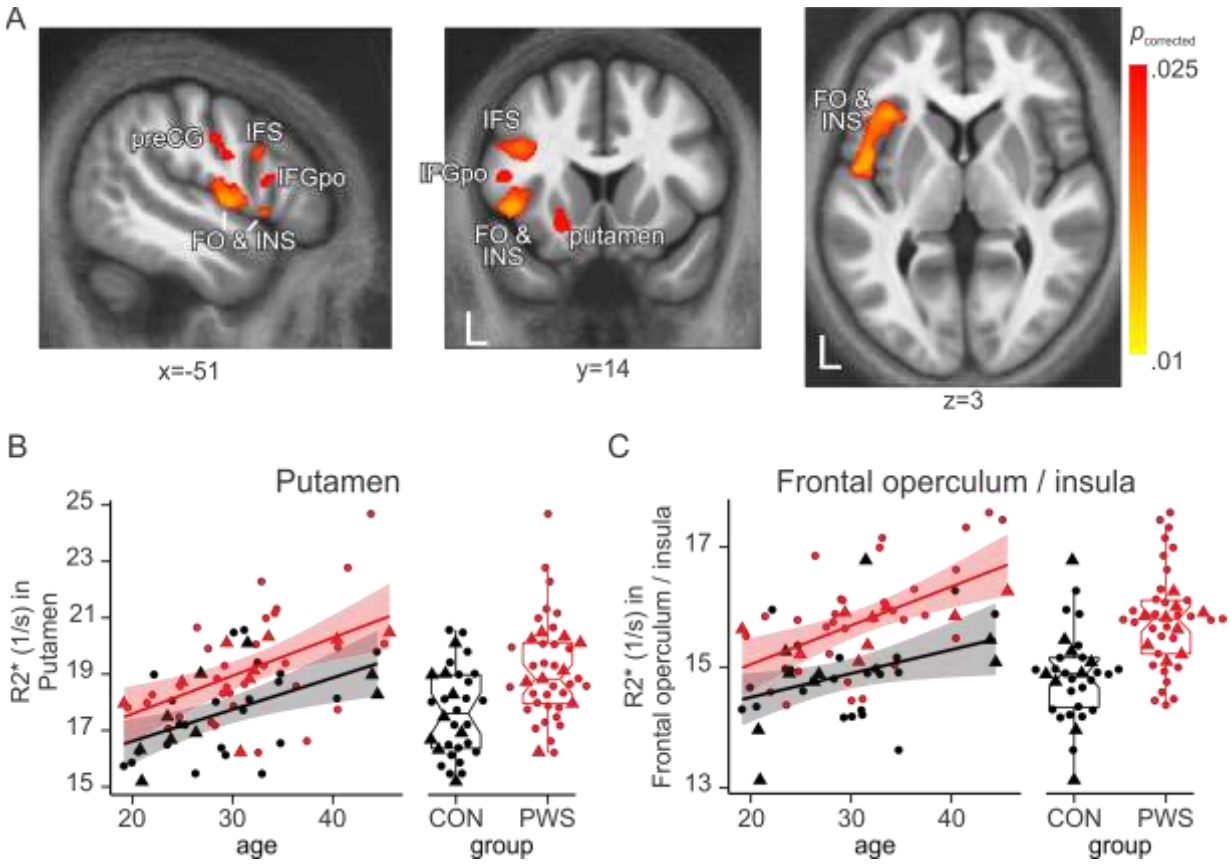

Figure 2. Areas with higher R2* in people who stutter relative to controls. (**A**) Coloured overlay is the statistical map showing areas with higher R2* in PWS than controls (thresholded at p<.025) on top of the average MTsat map for all participants aligned to MNI space. Individual data for mean R2* plotted against age by group in (**B**) left putamen (**C**) left frontal operculum and insula. Red is PWS; black is CON. Circles are men and triangles are women. Shaded areas show 95% confidence intervals. In boxplots, centre line is median and edges are 25th and 75th percentiles. Abbrev: L: left hemisphere; preCG: precentral gyrus; IFS: Inferior frontal sulcus (posterior); IFGpo: Inferior frontal gyrus, pars opercularis; FO & INS: Frontal operculum / insula

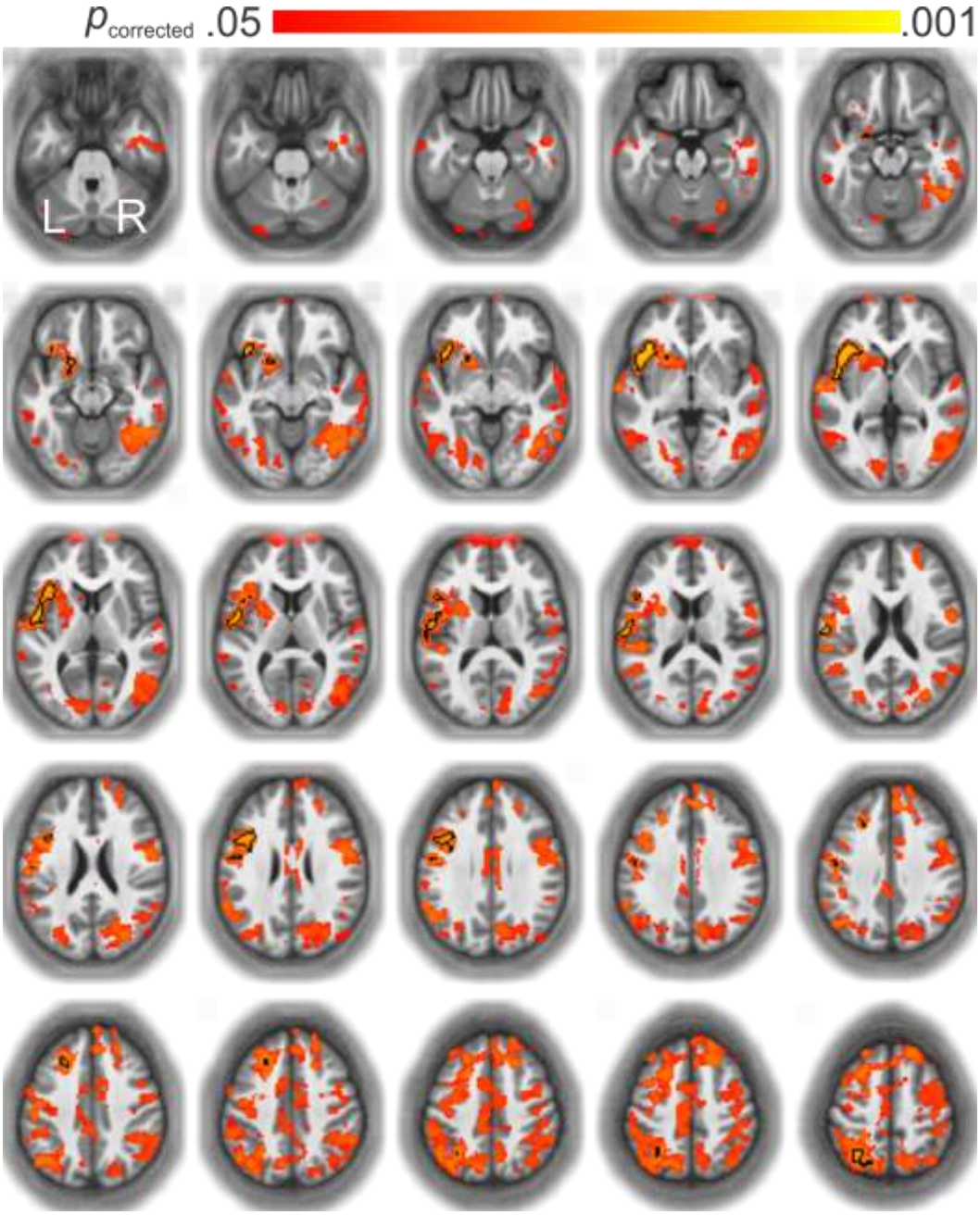

Supplemental Figure 1. Subthreshold areas with higher R2* in people who stutter relative to controls. Coloured overlay is the statistical map showing areas with higher R2* in PWS than controls in red-to-yellow thresholded at corrected p<.05. Statistically significant areas at a corrected threshold of p<.025 are outlined in black. Shown on top of the average MTsat map for all participants aligned to MNI space. L: left; R: right hemispheres.

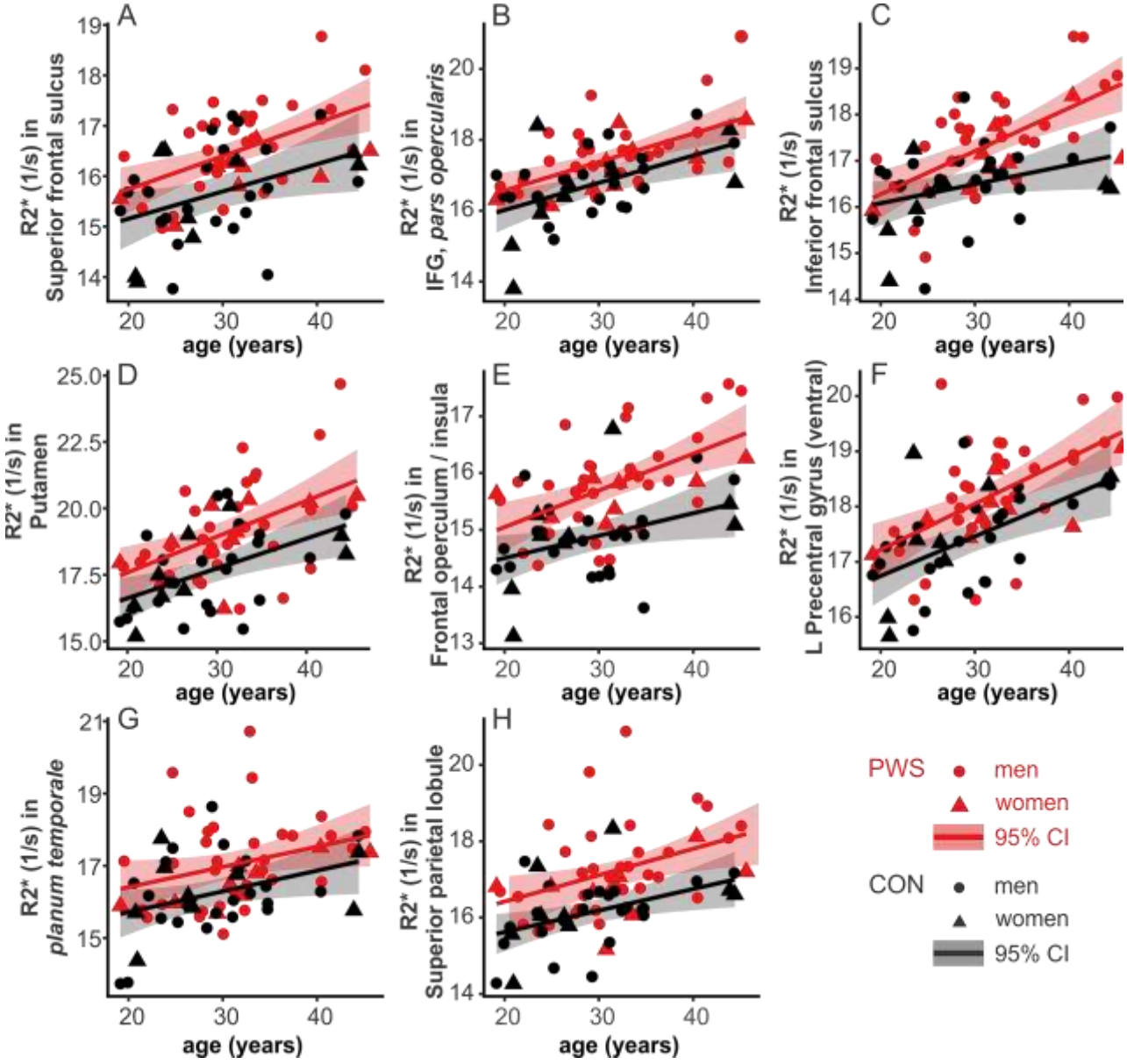

Supplemental Figure 2. Age and group effects on R2* in all areas with higher R2* in PWS than controls ($p < .025$). Associated statistical results are shown in Supplemental Table 1. Red is PWS; black is CON. Circles are men and triangles are women. Shaded areas show 95% confidence intervals. (**A**) L Superior frontal sulcus; (**B**) L Inferior frontal gyrus, *pars opercularis*; **(C)** L Inferior frontal sulcus (posterior); **(D)** L Putamen (same as *Figure 2*D); **(E)** L Frontal operculum / insula (same as *Figure 2*E); **(F)** L Precentral gyrus (ventral); **(G)** L planum temporale; **(H)** L Superior parietal lobule.

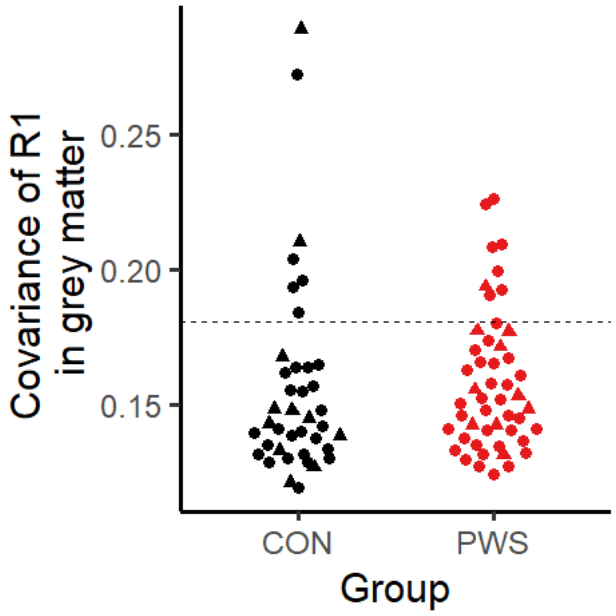

Supplemental Figure 3. Results of semi-automated quality control algorithm. CON shown in black on left; PWS shown in red on right. Circles are men and triangles are women. Quality control cutoff (dashed horizontal line) was chosen empirically to be consistent between groups and to separate acceptable from unacceptable movement. Only participants with grey matter covariance in R1 map ≤ .18 were included in all subsequent analyses. Data from three additional participants with acquisition artefacts were excluded and not shown here.

Table 1. Locations of increased R2* in PWS relative to CON

Brain Area	X	Y	Z	Voxels	*p*
L Superior frontal sulcus	-24	27	40	513	0.023
L Inferior frontal gyrus, *pars opercularis*	-49	15	14	229	0.024
L Inferior frontal sulcus (posterior)	-42	11	27	1677	0.019
L Putamen	-21	10	-11	615	0.023
L Frontal operculum / anterior insula	-46	8	3	6674	0.012
L Precentral gyrus (ventral)	-52	-6	29	499	0.024
L Planum temporale	-56	-30	15	6	0.025
L Superior parietal lobule	-28	-60	56	1626	0.018

Thresholded at $p<.025$. Coordinates of the center of gravity of each cluster are provided in MNI152 space. The extent of each cluster is provided in voxels. The p-value for the peak voxel is shown in the final column.

Supplemental Table 1. Parameters for each tissue type across the whole brain.

Parameter	Med (SE) CON	Med (SE) PWS	Age		Group		Age × group	
			F	*p*	*F*	*p*	*F*	*p*
R1 – white matter	0.9 (.005)	0.9 (.004)	7.4	**0.008**	1.5	0.2	2.2	0.1
R1 – grey matter	0.7 (.003)	0.7 (.002)	15.2	**<0.001**	0.4	0.5	0.0	0.9
MT – white matter	1.6 (.008)	1.5 (.007)	1.1	0.3	0.0	0.9	1.8	0.2
MT – grey matter	0.9 (.004)	0.9 (.003)	9.0	**0.004**	0.8	0.4	0.1	0.8
R2* – white matter	20.9 (.15)	21.0 (.10)	16.6	**<0.001**	0.1	0.8	2.2	0.1
R2* – grey matter	17.8 (.14)	18.0 (.13)	36.0	**<0.001**	3.3	0.1	0.0	0.9
Whole brain volume	1545506 (29660)	1579228 (17909)	0.3	0.6	0.8	0.4	0.4	0.5

Median and standard error for each parameter and tissue type across the whole brain. Differences tested statistically with analyses of variance (R command: aov) with factors of age, group, and age × group

Supplemental Table 2. Effects of age on R2* in statistical clusters; no interaction between age and group

Brain region	Med (SE) CON	Med (SE) PWS	Age		Group		Age × group	
			F	*p*	*F*	*p*	*F*	*p*

L Superior frontal sulcus	15.7 (0.17)	16.5 (0.13)	25.5	**<0.001**	13.3	**0.001**	0.2	0.7
L Inferior frontal gyrus, *pars opercularis*	16.7 (0.18)	17.4 (0.15)	35.4	**<0.001**	8.3	**0.005**	0.01	0.9
L Inferior frontal sulcus (posterior)	16.5 (0.15)	17.5 (0.16)	32.5	**<0.001**	14.3	**<0.001**	3.5	0.07
L Putamen	17.6 (0.27)	18.8 (0.28)	31.2	**<0.001**	11.7	**0.001**	0.2	0.7
L Frontal operculum / insula	14.9 (.13)	15.8 (.13)	28.8	**<0.001**	23.7	**<0.001**	1.1	0.3
L Precentral gyrus (ventral)	17.4 (0.16)	18.1 (0.15)	41.0	**<0.001**	10.0	**0.002**	0.2	0.7
L Superior parietal lobule	16.2 (0.16)	17.1 (0.18)	19.9	**<0.001**	15.5	**<0.001**	0.1	0.7
L planum temporale	16.2 (0.2)	17.0 (0.19)	11.9	**0.001**	6.5	**0.01**	<0.01	1

Median and standard error (SE) for R2* in grey matter in statistical clusters (p<.025) for people who stutter (PWS) and controls (CON). Differences tested statistically with analyses of variance (R command: aov) accounting for age, group, and age × group.

Supplemental Table 3. No effect of severity on R2* in PWS

Brain region	**Age**		**Severity**		**Age × severity**	
	F	***p***	***F***	***p***	***F***	***p***
L Superior frontal sulcus	13.9	**0.001**	0.1	0.7	0.0	1.0
L Inferior frontal gyrus, *pars opercularis*	17.2	**<0.001**	0.9	0.4	0.0	0.9
L Inferior frontal sulcus (posterior)	23.7	**<0.001**	1.2	0.3	0.4	0.5
L Putamen	13.1	**0.001**	0.1	0.7	1.1	0.3
L Frontal operculum / insula	15.8	**<0.001**	2.6	0.1	0.1	0.8
L Precentral gyrus (ventral)	20.1	**<0.001**	3.7	0.06	0.1	0.7
L planum temporale	4.1	**0.05**	0.5	0.5	0.9	0.3
L Superior parietal lobule	7.0	**0.01**	1.0	0.3	0.3	0.6